Molecular Cell
Article

Allosteric Signaling and a Nuclear Exit Strategy: Binding of UL25/UL17 Heterodimers to DNA-Filled HSV-1 Capsids

Benes L. Trus,[1,2,5] William W. Newcomb,[3,5] Naiqian Cheng,[1,5] Giovanni Cardone,[1,5] Lyuben Marekov,[1] Fred L. Homa,[4] Jay C. Brown,[3] and Alasdair C. Steven[1,*]
[1] Laboratory of Structural Biology Research, National Institute of Arthritis and Musculoskeletal and Skin Diseases
[2] Imaging Sciences Laboratory, Division of Computational Bioscience, Center for Information Technology
National Institutes of Health, Bethesda, MD 20892, USA
[3] Department of Microbiology and Cancer Center, University of Virginia Health System, Charlottesville, VA 22908, USA
[4] Department of Molecular Genetics and Biochemistry, University of Pittsburgh School of Medicine, Pittsburgh, PA 15261, USA
[5] These authors contributed equally to this work.
*Correspondence: alasdair_steven@nih.gov
DOI 10.1016/j.molcel.2007.04.010

SUMMARY

UL25 and UL17 are two essential minor capsid proteins of HSV-1, implicated in DNA packaging and capsid maturation. We used cryo-electron microscopy to examine their binding to capsids, whose architecture observes T = 16 icosahedral geometry. C-capsids (mature DNA-filled capsids) have an elongated two-domain molecule present at a unique, vertex-adjacent site that is not seen at other quasiequivalent sites or on unfilled capsids. Using SDS-PAGE and mass spectrometry to analyze wild-type capsids, UL25 null capsids, and denaturant-extracted capsids, we conclude that (1) the C-capsid-specific component is a heterodimer of UL25 and UL17, and (2) capsids have additional populations of UL25 and UL17 that are invisible in reconstructions because of sparsity and/or disorder. We infer that binding of the ordered population reflects structural changes induced on the outer surface as pressure builds up inside the capsid during DNA packaging. Its binding may signal that the C-capsid is ready to exit the nucleus.

INTRODUCTION

Assembly and packaging of the nucleocapsid of herpes simplex virus is a complex, multistep process involving the coordinated activity of some 15 viral proteins (Baines and Duffy, 2006). Mechanistically, this pathway has much in common with capsid assembly of the tailed bacteriophages, suggesting common albeit distant evolutionary origins (Bamford et al., 2005; Steven et al., 2005; Baker et al., 2005). The capsid is first assembled as a precursor particle or procapsid into which DNA is then packaged. The procapsid's surface shell is composed of hexamers and pentamers of the major capsid protein, UL19 (VP5), coordinated by triplexes of UL18 (VP23) and UL38 (VP19c) (Newcomb et al., 1993), with the UL6 portal at one vertex (Newcomb et al., 2001). Subsequently, the procapsid undergoes a major transition—maturation—involving profound structural and compositional changes (Newcomb et al., 1996; Trus et al., 1996) (Figure 1). Its shape switches from spherical to polyhedral as the hexamers are remodeled (Heymann et al., 2003), such that a continuous inner "floor" layer is formed and sites are created around their outer tips to which the small protein UL35 (VP26) may bind (Booy et al., 1994; Zhou et al., 1995). Maturation is preceded by proteolytic cleavage of the internal scaffolding proteins. Because procapsids mature in vivo shortly after assembly, they are rarely captured in thin section electron micrographs of infected cells, but three capsids are observed in and may be isolated from the nuclei of infected cells: DNA-containing C-capsids and two capsids that lack DNA—B-capsids, which retain the scaffolding protein, and A-capsids, which do not. All three have mature shells. The latter two capsids appear to be aberrant byproducts, probably resulting from failure to complete (A-capsids) or to properly initiate (B-capsids) DNA packaging.

In addition to the components listed above, several other viral proteins interact with the capsid during DNA packaging and/or in readying the nucleocapsid to exit from the nucleus. UL15, UL28, and UL33 are components of the terminase—the enzyme that recognizes and cleaves at specific sites on the replicating concatemer of viral DNA and translocates DNA into the capsid (Baines and Weller, 2005; Jacobson et al., 2006). UL17 and UL25 play roles in DNA maturation and packaging (Salmon and Baines, 1998). Some light has been cast by experiments with viruses deleted for these genes. In the absence of UL17, the replicating DNA concatemer is not cleaved to genome-sized pieces, and DNA is not packaged (Thurlow et al., 2005). The absence of UL25 is less prohibitive (Stow, 2001): packaging takes place, but this DNA does not appear to be stably encapsidated, fewer C-capsids

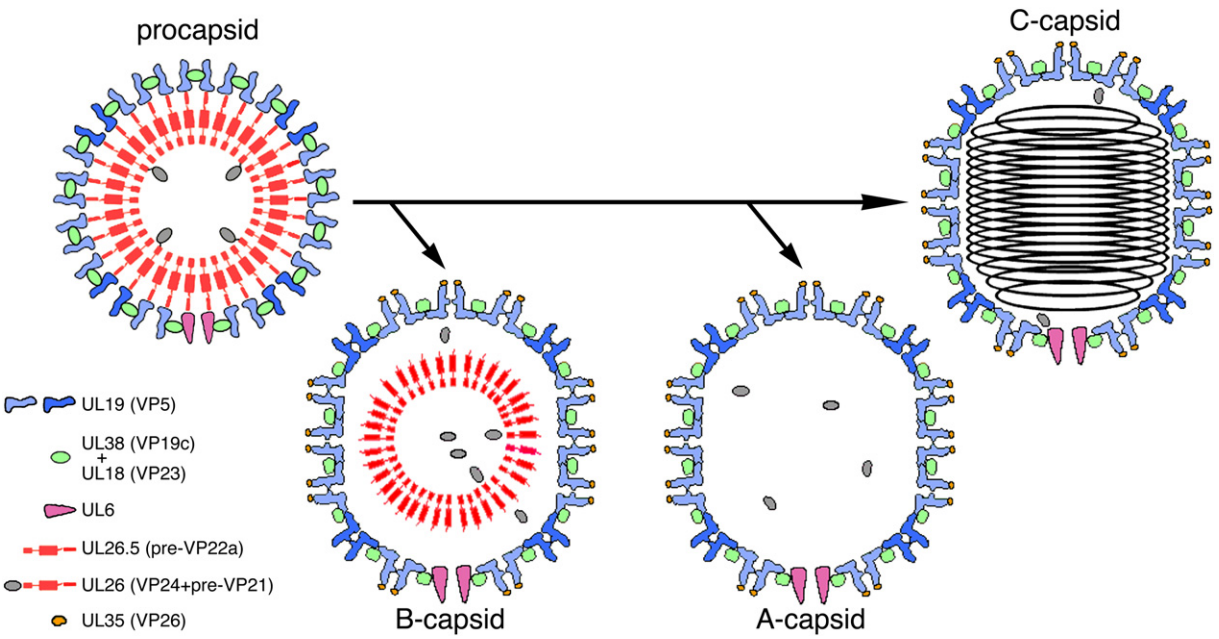

Figure 1. Alternative Maturation Pathways for the HSV-1 Procapsid

The procapsid surface shell is made up of hexamers (light blue subunits) and pentamers (midblue) of UL19, coordinated by triplexes, which are heterotrimers of UL18 and UL38. Its inner shell is composed of the scaffolding proteins UL26.5 and UL26. UL26 is an extended version of UL26.5, having the viral protease VP24 and a linker fused to its N terminus. A single dodecamer of UL6 is present at the portal vertex. In maturation, the protease is released by autoproteolysis and processes the C termini of the scaffolding proteins at the interface between the inner and outer shells. The surface shell then switches from round to polyhedral in shape, and UL35 binds to the outer tips of UL19 hexamers. The capsids are represented schematically in cross-sections that convey some, but not all, of their salient features.

being seen in the nuclei of infected cells (McNab et al., 1998). Observations on cells infected with a UL25 null mutant of pseudorabies virus (PRV, another α-herpesvirus) detected C-capsids inside but not outside the nucleus, implying that they are more stable than their HSV-1 counterparts but unable to embark on nuclear export (Klupp et al., 2006).

Previous studies have determined that UL17 and UL25 are incorporated into capsids in roughly equal amounts, estimated at 15–40 copies per capsid in B-capsids and A-capsids and somewhat more in C-capsids (see Table S2 in the Supplemental Data available with this article online). Absence of one protein (by mutation) impairs incorporation of the other, and when B-capsids are treated with increasing amounts of urea, the proteins are extracted in parallel (Thurlow et al., 2006). These observations suggest that they might form a complex. However, there is also evidence for noncoupled populations of these molecules (Thurlow et al., 2006).

Capsid-associated UL25 and UL17 are sensitive to trypsin (Newcomb et al., 2006; Wills et al., 2006), indicating that they are exposed on the outer surface, an inference corroborated by EM studies demonstrating that anti-UL25 and anti-UL17 antibodies bind to the capsid exterior (Newcomb et al., 2006; Thurlow et al., 2006).

Motivated by the prospect that identifying the capsid locations of UL25 and UL17 might yield insight as to their function(s), we have approached this problem by cryo-EM and image reconstruction, complemented with biochemical analysis. Initially, we focused on C-capsids, which have the highest content of UL25. For reference, we also analyzed unfilled capsids (A-capsids) from a UL25 null mutant and from the wild-type virus. These studies visualized an additional structural component present on C-capsids but not on any other capsid examined: we refer to it as the C-capsid-specific component (CCSC). Correlation of its presence with protein composition was not straightforward, as unfilled capsids also contain UL25 and UL17 but do not exhibit the CCSC. Nevertheless, combining our cryo-EM data with biochemical data and other observations led to the conclusion that the CCSC is a heterodimer of UL25 and UL17.

RESULTS

Detection of an Additional Component, the CCSC, on the Outer Surface of C-Capsids

C-capsids were isolated from the nuclear fraction of infected cells harvested at 20 hr postinfection. Examination by cryo-EM confirmed that the capsids were highly purified (data not shown). The resulting micrographs were used to calculate two independent reconstructions (Table 1). They consistently revealed an additional component—the CCSC—on the outer surface of the capsid (compare

Table 1. Presence of CCSC in Cryo-EM Reconstructions of HSV-1 Capsids

Type of Capsid	Resolution (Å)[a]	Number of Particles	CCSC Occupancy[b]	Copy Number
C-capsids	19.9 (0.5) 17.6 (0.3)	643 pairs	0.54, 0.55 (**0.55**)	33
C-capsids	26.8 (0.5) 24.5 (0.3)	538	0.45, 0.44 (**0.45**)	27
A-capsids (wild-type)[c]	22.9 (0.5)	2111	0.15, 0.07 (**0.11**)	7
A-capsids (wild-type)[c,d]	27.5 (0.5) 26.8 (0.3)	1100	0.18, 0.08 (**0.13**)	8
A-capsids (UL25 null)	22.7 (0.5) 21.9 (0.3)	1088	0.00, 0.00 (**0.00**)	0
C-capsids (+0.5 M Guan.HCl)	25.0 (0.5) 24.1 (0.3)	595	0.00, 0.00 (**0.00**)	0

[a] Resolution is according to the Fourier Shell Correlation (Saxton and Baumeister, 1982), thresholded at 0.5 or 0.3.
[b] The two numbers correspond to measurements made in the vertex-distal and the vertex-proximal parts of the CCSC and, in bold, their mean.
[c] Reported by Cheng et al. (2002).
[d] In this reconstruction, grayscale sections show some faint density at the CCSC site, but it is at the level of background noise. If genuine, it would correspond to an occupancy 3-fold to 4-fold lower than is observed on C-capsids.

Figures 2B and 2A). This molecule is ~14 nm long by ~3 nm wide and appears to consist of two domains. It interacts with the two triplexes closest to the UL19 penton (triplexes Tc and Ta, in the nomenclature of Zhou et al. [1994]), makes glancing contact with the adjacent UL19 hexamer (the P hexon, in the nomenclature of Steven et al. [1986]), and extends toward the UL19 penton (Figure 2C). The molecule is visibly present only at this site (apart from repetitions generated by icosahedral symmetry) and not at any of the other quasiequivalent sites that are distributed over the capsid surface (Figures 2B and 3A).

The CCSC is also evident in grayscale sections (arrows, Figures 2E, 3A, and 4A). Its average occupancy may be estimated in terms of the value of its peak density relative to that in the capsid shell (assumed to be 100% occupancy) and the average density outside the capsid (0% occupancy). In this way, we measured the average occupancy of the CCSC to be 50% ± 5%, corresponding to an average copy number of 30 per capsid (0.5 × 60) (Table 1).

The CCSC Is Not Seen on UL25 Null A-Capsids

Because our working hypothesis was that it might be possible to visualize UL25 on C-capsids (see the Introduction), we also analyzed capsids from a UL25 null deletion mutant as a negative control. However, we have not been able to recover C-capsids from this mutant. Accordingly, bearing in mind that wild-type A-capsids also contain UL25 (Newcomb et al., 2006), we isolated UL25 null A-capsids and analyzed them by cryo-EM. The capsid structure, otherwise normal, shows no trace of the CCSC (Figures 2A and 2D).

The CCSC Is Not Seen on Wild-Type A-Capsids

The CCSC has not been reported in previous cryo-EM studies of A-capsids or B-capsids. Accordingly, to clarify the significance of its absence from UL25 null A-capsids, we scrutinized two reconstructions of wild-type A-capsids in the vicinity of the CCSC binding site but observed no significant density there (Figure 4C, Table 1).

Minor Capsid Proteins Detected by Biochemical Analysis

In Figure 5, we compare the protein compositions of wild-type C-capsids, A-capsids, and virions, as resolved by SDS-PAGE with Coomassie blue staining. Also compared are wild-type A-capsids and A-capsids from the UL25 null mutant. The gels confirm the high degree of purity of these preparations. The major proteins—UL19, UL38, and UL18—contribute strong bands. The C-capsids show only three additional, much less intense, bands in the region between UL19 and UL38. We used mass spectrometry to identify them as UL17 (band c-1), UL6 (band c-2), and UL25 (band c-3) —Table S1 and Figure S1. The UL25 and UL17 bands are also present in A-capsids: although even weaker than in C-capsids, they are in the same relative amounts, i.e., the UL25 band is somewhat stronger. The faint UL6 band is of the same intensity in both capsids—as expected, since each should contain a single dodecamer of this protein. The UL25 band is indeed missing from UL25 null A-capsids (Figure 5, right panels).

The intensities of these gel bands were used to estimate the copy numbers of UL25 and UL17. These quantitations were calibrated relative to both triplex proteins, yielding copy numbers of 82 ± 19 (UL25) and 36 ± 8 (UL17) for C-capsids (Table S2).

The protein composition of virions is considerably more complex than those of capsids (Gibson and Roizman [1972] and Figure 5). Because the UL36 (VP1-3) protein has been invoked as a prominent component attached to the capsid outer surface in virions (Zhou et al. [1999]; see the Discussion), we sought to identify the corresponding band by mass spectrometry. It is the most intense of the several high-MW bands in the virion lane (band v-1 in Figure 5; see Figure S1 and Table S1). In contrast, there is essentially no staining at this position in the C-capsid or A-capsid lanes (Figure 5). From these data, we put the VP1-3 content of C-capsids, if any, at less than one molecule per capsid.

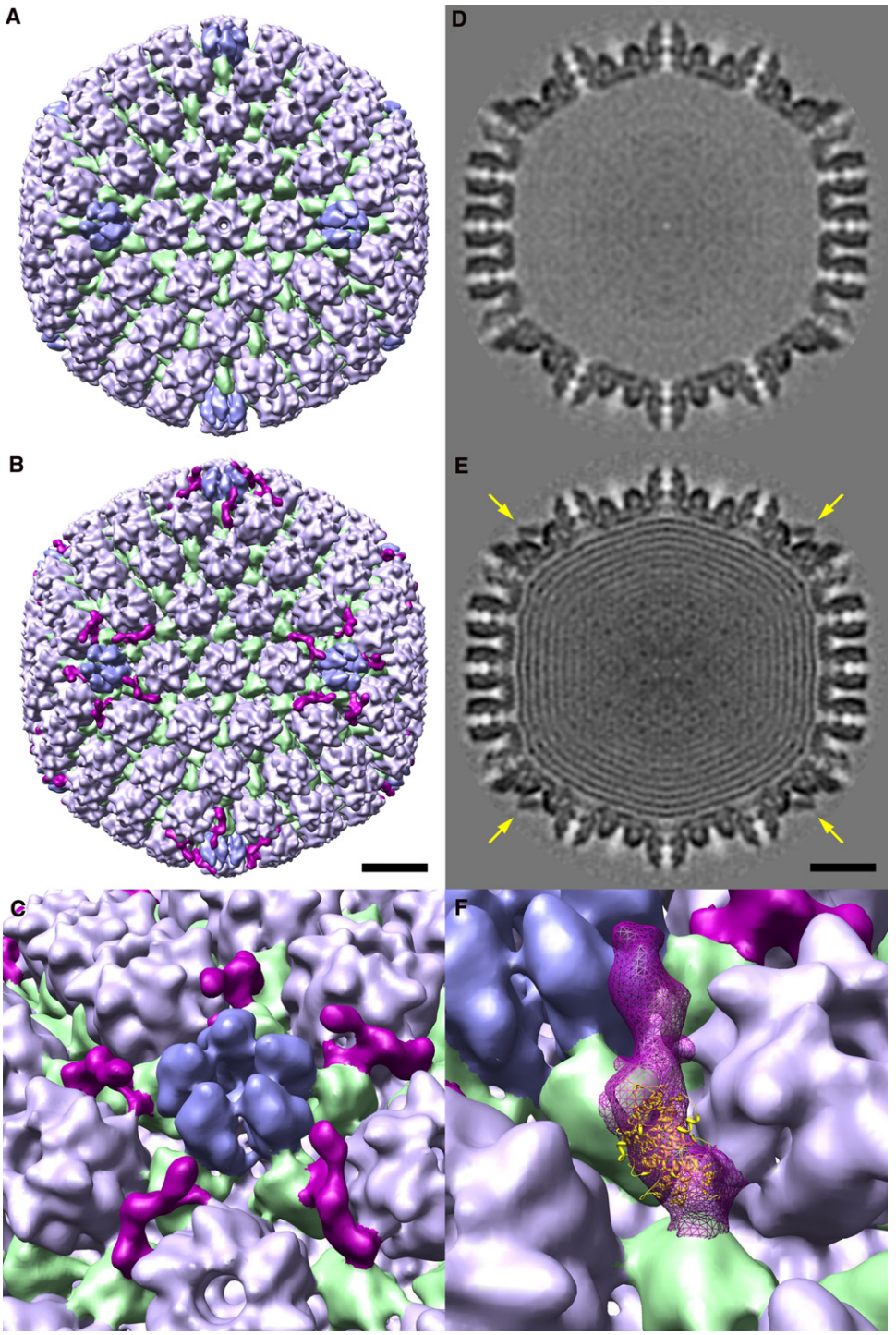

Figure 2. The CCSC Is Present on C-Capsids but Not on UL25 Null A-Capsids

Surface renderings of cryo-EM reconstructions are shown in (B) (C-capsid) and (A) (UL25 null A-capsid). Triplexes are green, hexons (UL19 hexamers with six VP26 molecules around their outer tip) are light blue, and pentons (UL19 pentamers) are midblue. The CCSC in (B) is purple. The capsids are viewed along a 2-fold axis of icosahedral symmetry. (C) shows a blow-up of the region around a penton, presenting five different views of the CCSC molecules clustered around this vertex. Scale bar in (B) and (E), 20 nm. (D) and (E) show central sections of the two capsids. High density is dark. The UL25 null A-capsid is empty; the C-capsid contains nested shells of DNA (Booy et al., 1991). Arrows in (E) point to the CCSC, which is sampled in this plane. (F) shows the optimal fit of a UL25 fragment into the CCSC.

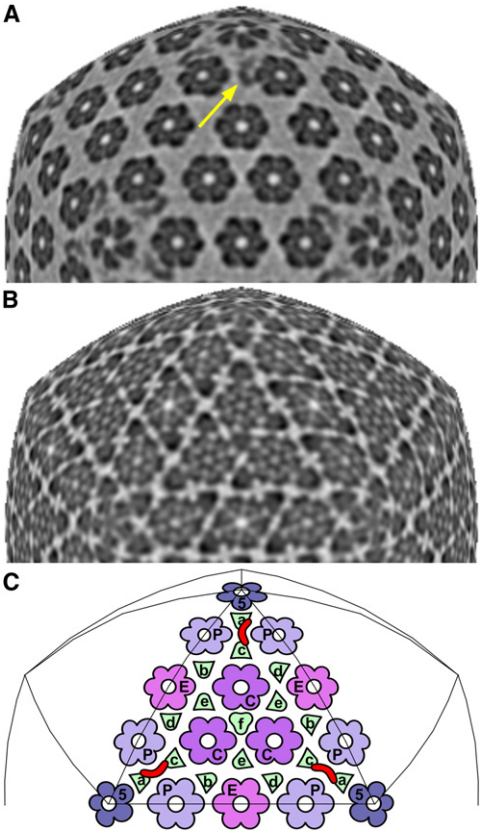

Figure 3. The CCSC Is Visible at Only One of Six Quasiequivalent Sites on the HSV-1 C-Capsid

(A) and (B) show icosahedral sections through the C-capsid at radii of 61 and 53 nm, respectively, along the 3-fold axis. In them, the sampling surface maintains the same radial position relative to the capsid shell (as opposed to the capsid center). (A) is rescaled so that features in it line up with underlying features in (B). (A) samples the CCSC (yellow arrow), whereas (B) samples the triplexes as well as the capsomer protrusions, just above the floor. In (C) are mapped the positions of the four kinds of capsomers and six kinds of triplexes on one triangular facet. Each CCSC (marked in red) overlies a pair of triplexes (Tc, Ta). Other quasiequivalent sites may be found by substituting another kind of triplex for Tc. There are 320 triplexes, but maximum CCSC binding would correspond to 160 copies, because one CCSC occludes two triplexes. The CCSC is seen on C-capsids at only one of the six possible sites, at 50% occupancy. This occupancy may increase in virions, whose UL25 content is higher than that of C-capsids (Thurlow et al., 2006).

Extraction of UL25 and UL17 from C-Capsids

The copy numbers of UL25 and UL17 in C-capsids estimated by biochemical analysis are more than sufficient to match the number of CCSC molecules determined by cryo-EM. Conversely, UL25 null A-capsids have zero (UL25) or very small (UL17) contents of these proteins by SDS-PAGE (Figure 5), and the CCSC is absent by cryo-EM (Figure 2). However, the significance of the latter correlation is clouded by the absence of the CCSC from wild-type A-capsids that contain these proteins. It appeared, therefore, that the presence of the CCSC on C-capsids might depend on their having encapsidated DNA. To explore this hypothesis, we tested the effect of releasing their DNA by a relatively mild treatment that otherwise leaves the capsid shell minimally perturbed. Treatment of C-capsids with 0.5 M guanidine hydrochloride (Guan.HCl) has this effect (Newcomb and Brown, 1994).

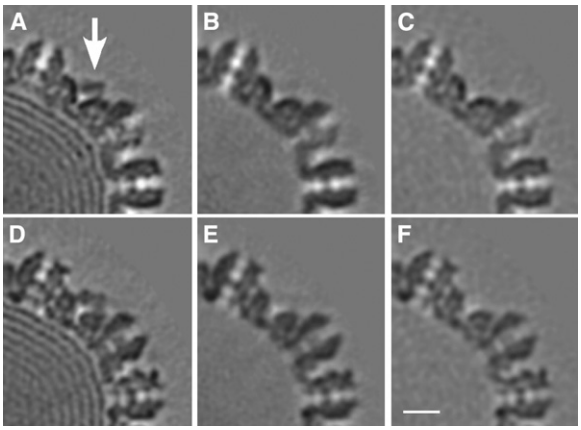

Figure 4. The CCSC Is Removed from C-Capsids by 0.5 M Guan.HCl and Is Absent from Wild-Type A-Capsids

(A and D) Two sections from a C-capsid reconstruction in which the CCSC is sampled (arrow). (B and E) Corresponding sections from C-capsids after treatment with 0.5 Guan.HCl. Note the absence of both the DNA and the CCSC. (C and F) Corresponding sections from a reconstruction of wild-type A-capsids. Scale bar, 10 nm.

After a 30 min incubation of C-capsids with 0.5 M Guan.HCl, they were separated from the denaturant and examined by cryo-EM for the CCSC, as well as biochemically for the presence of UL25 and UL17. Almost all capsids were either empty or retained only vestigial amounts of DNA. Image reconstruction revealed that they retained no detectable amounts of the CCSC (Figures 4B and 4E; Table 1). A control reconstruction of C-capsids from the same preparation that were treated identically, apart from omitting the Guan.HCl, confirmed that they contained the CCSC (data not shown). That the capsid shells were otherwise minimally perturbed was attested by their retention of UL35, which is known to be relatively easily detached (Newcomb et al., 1993). Their UL35 was visible as characteristic "horns" around the tips of the UL19 hexons, but not the pentons (data not shown, compare Figure 2C).

According to quantitative Western analysis, these C-capsids lost ~69% of their UL25 and a similar fraction (~59%) of their UL17 as a result of treatment with 0.5 M Guan.HCl.

Taken together, therefore, the cryo-EM observations and the biochemical data support the view that the CCSC is a heterodimer of UL25 and UL17.

Docking the Crystal Structure of a UL25 Fragment into the CCSC

The C-terminal portion of UL25, residues 134–580, has been crystallized and its structure determined (Bowman

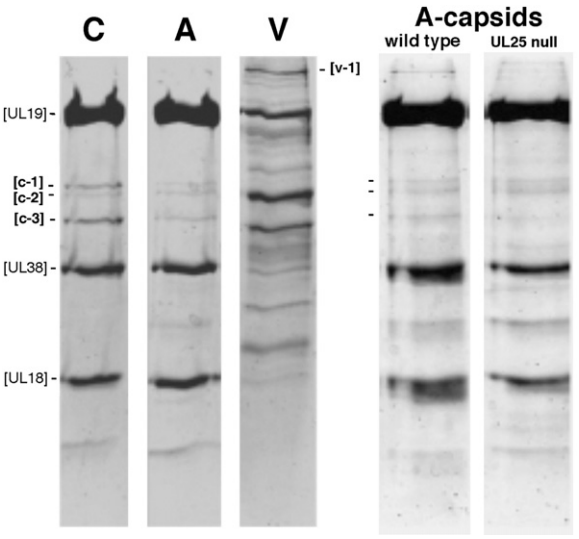

Figure 5. Identification of Minor Protein Components of HSV-1 Capsids

At left, C-capsids (C), wild-type A-capsids (A), and virions (V) are compared by SDS-PAGE with Coomassie blue staining. Equal amounts of protein were loaded in each lane. The major capsid proteins, UL19, UL38, and UL18, contribute strongly staining bands. The weak bands, c1, c-2, and c-3, were identified by mass spectrometry as UL17, UL6, and UL25, respectively. The v-1 band was identified as UL36. At right, wild-type A-capsids are compared with A-capsids from a UL25 null mutant. Again, c1, c-2, and c-3 are marked. The mutant capsids do not contain UL25, as confirmed by Western blotting (McNab et al., 1998). The very faint band running just below the UL25 position in the UL25 null mutant lane represents an unknown contaminant.

et al., 2006). We tried docking this fragment (Protein Data Bank ID code 2F5U), which is a monomer of ~5.5 × 3.5 × 4 nm, into the molecular envelope of the CCSC. Its volume, which we estimate as 122 nm^3, corresponding to a mass of ~100 kDa, is too large for a monomer of either UL25 (63 kDa; the solved crystal structure has a mass of 44 kDa) or UL17 (75 kDa). The most plausible interpretation, in view of their copy numbers, is that the two lobes of the CCSC should accommodate, respectively, monomers of these two proteins. We tried docking UL25 into both lobes and in both orientations. The docking was performed both manually and with an automated docking program. In both cases, the most satisfactory fit was obtained with the UL25 fragment in the lobe that is distal to the adjacent 5-fold axis, oriented as shown in Figure 2D. There, its center of mass is ~14 nm from the closest 5-fold axis and ~23 nm from the closest 3-fold axis of the capsid.

DISCUSSION

We have visualized the CCSC—an elongated molecule, comprising at least two domains or subunits—on the outer surface of C-capsids (Figures 2 and 3). Its primary points of contact are on the two triplexes closest to a vertex. There are no visible indications of its presence at other quasiequivalent sites (Figures 2B, 3A, and 3C). Correlation of biochemical data with structural data affords persuasive evidence that the CCSC is a heterodimer of UL25 and UL17. However, these proteins are also present in lower but comparable amounts on unfilled capsids, i.e., A-capsids and B-capsids, on which the CCSC is not seen. To reconcile these observations, we infer that there are two populations of capsid-associated UL25 and UL17 molecules: the visible population seen on C-capsids and populations that are invisible in averaged density maps but are nevertheless present on A- and B-capsids as well as on C-capsids. In the following, we discuss this scenario and its implications.

The CCSC Is Not Seen on Unfilled Capsids

In this context, it is noteworthy that, in immunogold EM labeling experiments of intracellular PRV capsids with anti-UL25 antibodies, Klupp et al. (2006) observed labeling of C-capsids but not of A-capsids or B-capsids. Based on the present results, we suspect that their antibodies were conformationally sensitive, specifically recognizing UL25 in the PRV version of the CCSC.

The CCSC Is Present in Virions and Is Not UL36 (VP1-3)

We reproducibly observed the CCSC in C-capsid reconstructions. In retrospect, it is also discernible in our earlier C-capsid reconstruction, despite its lower resolution (Booy et al., 1991). Like C-capsids, capsids inside virions are fully packaged with DNA. Consistent with this trend, the CCSC appears to be present in the nucleocapsid reconstructed from intact enveloped virions by Zhou et al. (1999). In this comparison—compare Figure 2 with Figure 2 of Zhou et al. (1999)—allowance should be made for the fact that the capsid in the latter reconstruction has a different hand. (The hand of the HSV-1 capsid was determined later in an EM tilting experiment [Cheng et al., 2002].) The inferred interaction of UL25 with the capsid inside virions is supported by the observation that it remains capsid associated when virions are extracted with Triton X-100 (Wolfstein et al., 2006).

Zhou et al. (1999) assigned this feature of their reconstruction as part of a single protein, UL36—a large tegument component of 335 kDa. However, as our C-capsids are devoid of UL36, that assignment is inapplicable. We posit that three proteins contribute to this feature: the two lower lobes are monomers of UL25 and UL17. The CCSC-like feature in virions extends further on to the penton crown than does its counterpart on C-capsids. (Penton-crowning density has also been detected on intraviral nucleocapsids by cryo-electron tomography—Grünewald et al. [2003].) The latter density may represent a small portion of UL36, but this proposition remains unproven.

Evidence for Two Populations of UL25 and UL17

It is difficult to measure the copy numbers of minor components of such complex particles as HSV-1 virions and

capsids with high precision by SDS-PAGE. Nevertheless, estimates have been made for UL25 and UL17 by several investigators, with fair consistency (Table S2). Taken together, these data support the following view: (1) both proteins are present in wild-type A-capsids and B-capsids in copy numbers of ~15–40 per capsid (different batches of A-capsids appear to be more variable in this respect than B-capsids—W.W.N., unpublished data); (2) both proteins have higher contents in C-capsids, corresponding to ~50–80 copies of UL25 per capsid; (3) all capsids have somewhat more UL25 than UL17.

From cryo-EM, we obtained an average of ~30 copies of the CCSC per C-capsid. The CCSC is too large for a monomer of either protein, and its shape does not subdivide into equal parts so as to suggest that it is a homodimer or a homotrimer. Accordingly, the most likely explanation is that it is a heterodimer of UL25 and UL17. This proposal is consistent with prior observations indicating that the bindings of some UL25 and UL17 molecules to capsids are coupled, which in turn suggests that they interact (see the Introduction). As the crystal structure for a major fragment of UL25 fits well into the vertex-distal portion of the CCSC (Figure 2F), it follows that the vertex-proximal portion is likely to be UL17. This interpretation will be tested more conclusively if it proves possible to label the CCSC with anti-UL25 or anti-UL17 antibodies.

The average C-capsid should contain ~30 copies of both proteins, configured as CCSC molecules. According to the biochemical data (above), it should have additional populations of both proteins that are not seen in reconstructions. The latter resemble the populations that are present in A-capsids and B-capsids in size and (in)visibility. As noted above, the UL25 content appears to be somewhat greater than that of UL17 in all three capsids. The observed departure from equimolarity is not large and may simply reflect a difference in dye binding affinity and/or experimental uncertainties. However, there is also evidence that capsids can bind some UL25 molecules in the absence of UL17 partners and vice versa (Newcomb et al., 2006; Thurlow et al., 2006).

Where Are the Invisible Molecules Located, and Why Are They Invisible?

If they were at the same site as the CCSC and configured in the same way, UL25 and UL17 molecules are abundant enough in A-capsids and B-capsids to be seen in cryo-EM reconstructions (they would correspond to occupancies of 25%–66%). The occupancy threshold for visibility in a cryo-EM density map depends on the residual noise level that, in turn, depends on several factors including the number of particles included in the analysis. Acknowledging this variability, experience with the binding of Fab fragments to hepatitis B virus capsids (Conway et al., 2003) suggests that an occupancy of ~20% is a useful rule of thumb for a visibility threshold.

One explanation for the nonvisibility of UL25 and UL17 molecules in reconstructions of A- and B-capsids is that they may be scattered around other quasiequivalent sites. There are six variants of this site, if one counts by letting triplexes Ta, Tb, Td, Te, or Tf substitute for Tc in its CCSC binding role (Figure 3C). Altogether, there are 320 potential binding sites per capsid. If heterodimers of UL25 and UL17 were randomly distributed around these sites, the average occupancy would be <10% and thus below the threshold of detectability. A second possibility invokes disorder instead of sparsity. If single UL25 molecules—which may be in excess over UL17 (see above)—were to bind to triplexes but remain free to pivot around their point of attachment, they would be seen poorly, if at all, in a reconstruction, even with relatively high occupancy. Third, it is not ruled out that some UL25 and/or UL17 molecules engage in an entirely different mode of binding.

Allosteric Regulation of CCSC Binding: A Precedent in UL35 (VP26) Binding

To account for the presence of the CCSC only on C-capsids, we suggest that, as DNA packaging progresses and pressure from encapsidated DNA builds up on the inner surface of the capsid wall, it eventually reaches a point where a structural transition is elicited on the outer surface that affects the CCSC binding site, resulting in an enhanced affinity. The envisaged temporal control of CCSC binding in the maturation pathway by allostery has a precedent in the binding of UL35. The latter protein does not bind to the procapsid, but as the procapsid matures, the six protrusion domains of each UL19 hexon, initially splayed apart (Heymann et al., 2003), cluster into a 6-fold symmetric ring on which bipartite binding sites for UL35 monomers are created in the crevices between neighboring protrusions (Wingfield et al., 1997). In UL19 pentons, on the other hand, the protrusion domains remain apart so that UL35 binding sites are not created. This exclusion of UL35 from pentons leaves their crowns open to engage in other interactions (Chen et al., 2001).

Nature of the Allosteric Switch that Promotes CCSC Binding

The binding site of a CCSC molecule on the underlying capsid is tripartite, with contact points on the Ta triplex, the Tc triplex, and the sidewall of the P hexon. Our working hypothesis assigns the first and third of these contacts to UL25 and the second one to UL17, with the complex being further stabilized by the interface between UL25 and UL17. The inferred association of UL25 with a triplex is consistent with the report by Ogasawara et al. (2001) of an interaction with UL38 (VP19c). This arrangement—a network of interactions that appear, individually, to be rather weak but, collectively, consolidate the binding of the CCSC—is reminiscent of the situation pertaining to clathrin-coated vesicles (Wakeham et al., 2003).

The key transition in the maturation pathway is from the procapsid state to the C-capsid state, A- and B-capsids being abortive particles. On comparing the procapsid with the C-capsid (compare Figures 6A and 6B), two kinds of changes are seen to take place; the triplex structures are altered, as are the relative positions of the three CCSC

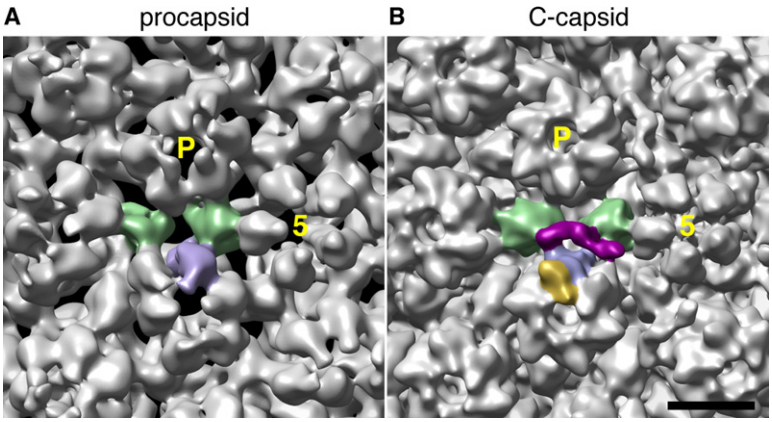

Figure 6. Changes Affecting the CCSC Binding Site on Maturation of the HSV-1 Procapsid

The regions of capsid surface surrounding the CCSC binding site are compared in cryo-EM reconstructions at ~2 nm resolution of the procapsid ([A], from Cheng et al. [2002]) and the C-capsid (B). In both cases, the two triplexes and one UL19 subunit that form the binding site for a single representative CCSC are shaded green and blue, respectively; this CCSC is purple in (B), and the UL35 subunit that tops the interacting UL19 subunit (but is not present on the procapsid) is gold. As reference points, the 5-fold axis of the adjacent UL19 penton is marked "5" and a neighboring P hexon with "P." Scale bar, 10 nm.

contact points. Maturation of the procapsid is a progressive event, proceeding through multiple intermediate states (Heymann et al., 2003). The final maturation step, undergone only by the C-capsid and crucial for CCSC binding, involves similar but smaller structural changes that bring the three contact points into juxtaposition (Movie S1). The relative importance of the two kinds of structural changes for CCSC binding will be clarified if it proves possible to extend the resolution of the procapsid and C-capsid significantly.

Functional Implications: Signaling and Nuclear Exit

At least two functions have been considered for UL25: stabilization of the DNA-filled capsid (Newcomb et al., 2006) and a role in nuclear exit (Klupp et al., 2006). It is noteworthy that the two triplexes to which the CCSC binds, Tc and Ta, are also the two that are most susceptible to extraction by denaturants, at concentrations (6M urea or 2M Guan.HCl) that also remove the pentons but otherwise respect the capsid framework (Newcomb et al., 1993).Thus, these triplex sites might be considered as weak points that are in need of reinforcement. However, since the CCSC is already extracted under less rigorous conditions (0.5 M Guan.HCl), it would not be still in place to provide reinforcement when denaturant concentrations rise to levels that threaten the Tc/Ta triplexes and the pentons. To the extent that resistance to denaturants is representative of the challenges against which the nucleocapsid needs to be stabilized, it is hard to see a role for the CCSC in this process. However, less extreme perturbations might also threaten the nucleocapsid, for instance, by causing it to lose its DNA, and CCSC binding might offer some protection against them.

The allosteric switch in the capsid shell that we infer to precede CCSC binding is reminiscent of signaling across a cell membrane (Alberts et al., 1989). In the latter case, an event on one side of the membrane, such as binding of a ligand to a receptor, elicits a downstream event on the other side, such as a phosphorylation cascade. In HSV-1 packaging, the signal comes from pressure imposed on the capsid inner surface by packaged DNA and elicits a structural change on the outer surface that facilitates CCSC binding.

It is tempting to envisage CCSC binding as a signal for nuclear export. Deferring this signal until late in packaging would avoid premature export of unpackaged or incompletely packaged capsids. It would also enhance overall replication efficiency for A-capsids and B-capsids—which remain within the nucleus—not to be allowed to embark on the tegumentation/envelopment pathway and therefore not committing further resources to the production of sterile particles. In this context, we note that UL36 is not needed for C-capsids to exit the nucleus but is required for them to achieve envelopment and exit the cytoplasm (Desai, 2000). The scenario outlined above relates to the observation by Thurlow et al. (2006) that virions contain twice as much UL25 as do nuclear C-capsids. This additional complement might represent an increase in average occupancy of the CCSC sites from ~50% to ~100%. Conversely, nuclear C-capsids may be still in the nucleus because they have not yet bound sufficient copies of the CCSC to enable their exit.

Noting that this scenario does not account for the phenotype of UL17 null mutants that fail to initiate DNA packaging (Salmon and Baines, 1998), we suggest that UL17 and possibly also UL25 may exercise additional functions earlier in the nucleocapsid assembly pathway.

With respect to other regulatory mechanisms that may be used to signal that packaging of nucleic acid into virus particles is at or approaching completion, Lander et al. (2006) have proposed a different allosteric mechanism, involving interaction of DNA with the portal, as a signal for termination of packaging into bacteriophage P22.

EXPERIMENTAL PROCEDURES

Preparation of Capsids

Wild-type C-capsids and A-capsids and UL25 null A-capsids were prepared as described (McNab et al., 1998; Newcomb et al., 2006).

Gel Electrophoresis and Western Blot Analyses

These assays were performed as described (Newcomb et al., 2006). The antibodies used in the immunoblotting experiments were

polyclonal antiserum raised against purified UL25 (McNab et al., 1998) and an anti-UL17 monoclonal, MAb 203 (Thurlow et al., 2006), a kind gift of Dr. V. Preston.

Extraction of C-Capsids with 0.5 M Guanidine Hydrochloride

Fifty microliters of 6 M Guan.HCl in TNE buffer (pH 7.5) was mixed with 440 μl of TNE and 10 μl of 1 M DTT followed by the addition of 100 μl of purified C-capsids at 0.5 mg/ml in TNE. After incubation on ice for 30 min, the solution was pelleted through a 20% sucrose cushion, supernatant was discarded, and the pellet was resuspended in 50 μl of TNE.

The fractions of UL25 and UL17 extracted were measured from a Western blot. The extracted capsids were solubilized and run on an SDS-PAGE gel, then blotted on to PVDF and stained with 1% Ponceau S (Newcomb et al., 2006). The blot was stained with monoclonal antibody 2D9 (1:2000 dilution) specific for UL25 as described (Sheaffer et al., 2001). The blot was then washed and restained with an anti-UL17 antibody (MAb 203).

Mass Spectrometry

Designated bands were excised from gels and extracted with 0.2 ml 50% (w/v) acetonitrile in 25 mM Tris-HCl (pH 8.1), followed by 0.2 ml 100% acetonitrile, and dried in vacuum. The gel pieces were rehydrated with 0.04 ml 20 μg/ml modified trypsin (Promega V5111) in 25 mM Tris-HCl (pH 8.1) and digested overnight at 37°C. Peptides were extracted with 0.1 ml 0.2% (w/v) trifluoroacetic acid, and extracts were freed from salts with zip-tip pipette tips (Millipore) and eluted with 3 μl 50 mM alfa-cyano-4-hydroxycinammic acid in 50% (v/v) acetonitrile/0.1% (w/v) TFA directly on the mass spectrometer sample plate.

Peptides were analyzed on an Applied Biosystems Voyager DE-Pro time-of-flight mass spectrometer in the reflectron mode. Internal mass calibration of raw spectra was performed with PeakErazor software (http://welcome.to/gpmaw/) on contaminant trypsin/keratin autolysis peaks. This resulted in mass accuracy <50 ppm in the subsequent mass search. Protein identification was performed on a locally run Mascot Search program (http://www.matrixscience.com/search_form_select.html) against the SProt/TrEMBL database.

Cryo-Electron Microscopy

Cryo-EM was performed as described (Cheng et al., 1999). Microscopy was performed, using low-dose procedures, at defocus values described below, on a CM200-FEG microscope (Philips, Eindhoven, The Netherlands). The same preparations of capsids were examined both by cryo-EM and by SDS-PAGE and mass spectrometry.

Three-Dimensional Image Reconstruction

Micrographs were digitized on an SCAI scanner (Z/I Imaging, Huntsville, AL) giving a pixel size of 3.68 Å. Particles were extracted and preprocessed with X3D (Conway et al., 1993), and contrast transfer function (CTF) parameters were estimated with Bsoft (Heymann and Belnap, 2007). CTF correction was performed by phase flipping. Defocus settings were such that the first CTF zeros were at $(20\ Å)^{-1}$ – $(24\ Å)^{-1}$ or $(16\ Å)^{-1}$ – $(20\ Å)^{-1}$ if a first exposure was taken. Initial estimates of the orientation angles were determined with the PFT algorithm (Baker and Cheng, 1996), starting from a pre-existing A-capsid reconstruction (Cheng et al., 2002) adjusted in scaling to match the current data. Refinements were performed with PFT2 (Bubeck et al., 2005). Density maps were calculated with EM3DR2 (http://people.chem.byu.edu/belnap/). For resolution assessment (Table 1), the radial zone between 42.7 and 67 nm was used.

Visualization and Molecular Modeling

Surface representations were produced by using Chimera (Goddard et al., 2005). Icosahedral sections (Böttcher et al., 1997) were calculated using a program of Dr. J.F. Conway. The pentons, hexons, and triplexes and the CCSC were automatically segmented using a flooding algorithm implemented in bsegment/Bsoft (Heymann and Belnap, 2007). Interfaces were checked visually and refined manually. The reconstructions were visualized at the threshold of one standard deviation. In the molecular modeling, the threshold was adjusted for the CCSC to take into account its lower occupancy.

The crystal structure of UL25 (Protein Data Bank ID code 2F5U) was docked manually using Chimera and the result checked by automated correlation-based fitting, with *colores* in the SITUS program (Chacon and Wriggers, 2002). All top-ranked solutions placed the UL25 fragment in the vertex-distal lobe of the CCSC.

Supplemental Data

Supplemental Data include one figure, two tables, one movie, and Supplemental References and can be found with this article online at http://www.molecule.org/cgi/content/full/26/4/479/DC1/.

ACKNOWLEDGMENTS

We thank Dr. J. Conway for providing his icosahedral section program, Drs. B. Heymann and D. Belnap for reconstruction software, and Dr. V. Preston for a gift of M203 antibody. This work was supported in part by the Intramural Research Programs of the National Institute of Arthritis and Musculoskeletal and Skin Diseases (NIAMS) and Center for Information Technology (CIT) and the National Institutes of Health (NIH) Intramural Targeted Antiviral Program (A.C.S.), and NIH grants to J.C.B. (AI41644-10) and F.L.H. (AI060836).

Received: January 12, 2007
Revised: March 16, 2007
Accepted: April 10, 2007
Published: May 24, 2007

REFERENCES

Alberts, B., Bray, D., Lewis, J., Raff, M., Roberts, K., and Watson, J. (1989). Molecular Biology of the Cell, Second Edition (New York: Garland Publishing Inc.), pp. 645–647.

Baines, J.D., and Weller, S.K. (2005). Cleavage and packaging of herpes simplex virus 1 DNA. In Viral Genome Packaging Machines, C. Catalano, ed. (New York: Kluwer Academic/Plenum Publishers).

Baines, J.D., and Duffy, C. (2006). Nucleocapsid assemby and envelopment of Herpes Simplex Virus. In Alpha Herpesviruses: Molecular and Cell Biology, R. Sandri-Goldin, ed. (Norwich, UK: Horizon Press).

Baker, T.S., and Cheng, R.H. (1996). A model-based approach for determining orientations of biological macromolecules imaged by cryoelectron microscopy. J. Struct. Biol. *116*, 120–130.

Baker, M.L., Jiang, W., Rixon, F.J., and Chiu, W. (2005). Common ancestry of herpesviruses and tailed DNA bacteriophages. J. Virol. *79*, 14967–14970.

Bamford, D.H., Grimes, J.M., and Stuart, D.I. (2005). What does structure tell us about virus evolution? Curr. Opin. Struct. Biol. *15*, 655–663.

Booy, F.P., Newcomb, W.W., Trus, B.L., Brown, J.C., Baker, T.S., and Steven, A.C. (1991). Liquid-crystalline, phage-like, packing of encapsidated DNA in herpes simplex virus. Cell *64*, 1007–1015.

Booy, F.P., Trus, B.L., Newcomb, W.W., Brown, J.C., Conway, J.F., and Steven, A.C. (1994). Finding a needle in a haystack: detection of a small protein (the 12-kDa VP26) in a large complex (the 200-MDa capsid of herpes simplex virus). Proc. Natl. Acad. Sci. USA *91*, 5652–5656.

Böttcher, B., Kiselev, N.A., Stel'Mashchuk, V.Y., Perevozchikova, N.A., Borisov, A.V., and Crowther, R.A. (1997). Three-dimensional structure of infectious bursal disease virus determined by electron cryomicroscopy. J. Virol. *71*, 325–330.

Bowman, B.R., Welschhans, R.L., Jayaram, H., Stow, N.D., Preston, V.G., and Quiocho, F.A. (2006). Structural characterization of the

UL25 DNA-packaging protein from herpes simplex virus type 1. J. Virol. *80*, 2309–2317.

Bubeck, D., Filman, D.J., Cheng, N., Steven, A.C., Hogle, J.M., and Belnap, D.M. (2005). Structure of the poliovirus 135S cell-entry intermediate at 10 Å resolution reveals the location of an externalized polypeptide that binds to membranes. J. Virol. *79*, 7745–7755.

Chacon, P., and Wriggers, W. (2002). Multi-resolution contour-based fitting of macromolecular structures. J. Mol. Biol. *317*, 375–384.

Chen, D.H., Jakana, J., McNab, D., Mitchell, J., Zhou, Z.H., Dougherty, M., Chiu, W., and Rixon, F.J. (2001). The pattern of tegument-capsid interaction in the herpes simplex virus type 1 virion is not influenced by the small hexon-associated protein VP26. J. Virol. *75*, 11863–11867.

Cheng, N., Conway, J.F., Watts, N.R., Hainfeld, J.F., Joshi, V., Powell, R.D., Stahl, S.J., Wingfield, P.E., and Steven, A.C. (1999). Tetrairidium, a four-atom cluster, is readily visible as a density label in three-dimensional cryo-EM maps of proteins at 10–25 Å resolution. J. Struct. Biol. *127*, 169–176.

Cheng, N., Trus, B.L., Belnap, D.M., Newcomb, W.W., Brown, J.C., and Steven, A.C. (2002). Handedness of the herpes simplex virus capsid and procapsid. J. Virol. *76*, 7855–7859.

Conway, J.F., Trus, B.L., Booy, F.P., Newcomb, W.W., Brown, J.C., and Steven, A.C. (1993). The effects of radiation damage on the structure of frozen hydrated HSV-1 capsids. J. Struct. Biol. *111*, 222–233.

Conway, J.F., Watts, N.R., Belnap, D.M., Cheng, N., Stahl, S.J., Wingfield, P.T., and Steven, A.C. (2003). Characterization of a conformational epitope on hepatitis B virus core antigen and quasiequivalent variations in antibody binding. J. Virol. *77*, 6466–6473.

Desai, P.J. (2000). A null mutation in the UL36 gene of herpes simplex virus type 1 results in accumulation of unenveloped DNA-filled capsids in the cytoplasm of infected cells. J. Virol. *74*, 11608–11618.

Gibson, W., and Roizman, B. (1972). Proteins specified by herpes simplex virus. 8. Characterization and composition of multiple capsid forms of subtypes 1 and 2. J. Virol. *10*, 1044–1052.

Goddard, T.D., Huang, C.C., and Ferrin, T.E. (2005). Software extensions to UCSF chimera for interactive visualization of large molecular assemblies. Structure *13*, 473–482.

Grünewald, K., Desai, P., Winkler, D.C., Heymann, J.B., Belnap, D.M., Baumeister, W., and Steven, A.C. (2003). Three-dimensional structure of herpes simplex virus from cryo-electron tomography. Science *302*, 1396–1398.

Heymann, J.B., and Belnap, D.M. (2007). Bsoft: image processing and molecular modeling for electron microscopy. J. Struct. Biol. *157*, 3–18.

Heymann, J.B., Cheng, N., Newcomb, W.W., Trus, B.L., Brown, J.C., and Steven, A.C. (2003). Dynamics of herpes simplex virus capsid maturation visualized by time-lapse cryo-electron microscopy. Nat. Struct. Biol. *10*, 334–341.

Jacobson, J.G., Yang, K., Baines, J.D., and Homa, F.L. (2006). Linker insertion mutations in the herpes simplex virus type 1 UL28 gene: effects on UL28 interaction with UL15 and UL33 and identification of a second-site mutation in the UL15 gene that suppresses a lethal UL28 mutation. J. Virol. *80*, 12312–12323.

Klupp, B.G., Granzow, H., Keil, G.M., and Mettenleiter, T.C. (2006). The capsid-associated UL25 protein of the alphaherpesvirus pseudorabies virus is nonessential for cleavage and encapsidation of genomic DNA but is required for nuclear egress of capsids. J. Virol. *80*, 6235–6246.

Lander, G.C., Tang, L., Casjens, S.R., Gilcrease, E.B., Prevelige, P., Poliakov, A., Potter, C.S., Carragher, B., and Johnson, J.E. (2006). The structure of an infectious P22 virion shows the signal for headful DNA packaging. Science *312*, 1791–1795.

McNab, A.R., Desai, P., Person, S., Roof, L.L., Thomsen, D.R., Newcomb, W.W., Brown, J.C., and Homa, F.L. (1998). The product of the herpes simplex virus type 1 UL25 gene is required for encapsidation but not for cleavage of replicated viral DNA. J. Virol. *72*, 1060–1070.

Newcomb, W.W., and Brown, J.C. (1994). Induced extrusion of DNA from the capsid of herpes simplex virus type 1. J. Virol. *68*, 433–440.

Newcomb, W.W., Trus, B.L., Booy, F.P., Steven, A.C., Wall, J.S., and Brown, J.C. (1993). Structure of the herpes simplex virus capsid. Molecular composition of the pentons and the triplexes. J. Mol. Biol. *232*, 499–511.

Newcomb, W.W., Homa, F.L., Thomsen, D.R., Booy, F.P., Trus, B.L., Steven, A.C., Spencer, J.V., and Brown, J.C. (1996). Assembly of the herpes simplex virus capsid: characterization of intermediates observed during cell-free capsid formation. J. Mol. Biol. *263*, 432–446.

Newcomb, W.W., Juhas, R.M., Thomsen, D.R., Homa, F.L., Burch, A.D., Weller, S.K., and Brown, J.C. (2001). The UL6 gene product forms the portal for entry of DNA into the herpes simplex virus capsid. J. Virol. *75*, 10923–10932.

Newcomb, W.W., Homa, F.L., and Brown, J.C. (2006). Herpes simplex virus capsid structure: DNA packaging protein UL25 is located on the external surface of the capsid near the vertices. J. Virol. *80*, 6286–6294.

Ogasawara, M., Suzutani, T., Yoshida, I., and Azuma, M. (2001). Role of the UL25 gene product in packaging DNA into the herpes simplex virus capsid: location of UL25 product in the capsid and demonstration that it binds DNA. J. Virol. *75*, 1427–1436.

Salmon, B., and Baines, J.D. (1998). Herpes simplex virus DNA cleavage and packaging: association of multiple forms of U(L)15-encoded proteins with B capsids requires at least the U(L)6, U(L)17, and U(L)28 genes. J. Virol. *72*, 3045–3050.

Saxton, W.O., and Baumeister, W. (1982). The correlation averaging of a regularly arranged bacterial cell envelope protein. J. Microsc. *127*, 127–138.

Sheaffer, A.K., Newcomb, W.W., Gao, M., Yu, D., Weller, S.K., Brown, J.C., and Tenney, D.J. (2001). Herpes simplex virus DNA cleavage and packaging proteins associate with the procapsid prior to its maturation. J. Virol. *75*, 687–698.

Steven, A.C., Roberts, C.R., Hay, J., Bisher, M.E., Pun, T., and Trus, B.L. (1986). Hexavalent capsomers of herpes simplex virus type 2: symmetry, shape, dimensions, and oligomeric status. J. Virol. *57*, 578–584.

Steven, A.C., Heymann, J.B., Cheng, N., Trus, B.L., and Conway, J.F. (2005). Virus maturation: dynamics and mechanism of a stabilizing structural transition that leads to infectivity. Curr. Opin. Struct. Biol. *15*, 227–236.

Stow, N.D. (2001). Packaging of genomic and amplicon DNA by the herpes simplex virus type 1 UL25-null mutant KUL25NS. J. Virol. *75*, 10755–10765.

Thurlow, J.K., Rixon, F.J., Murphy, M., Targett-Adams, P., Hughes, M., and Preston, V.G. (2005). The herpes simplex virus type 1 DNA packaging protein UL17 is a virion protein that is present in both the capsid and the tegument compartments. J. Virol. *79*, 150–158.

Thurlow, J.K., Murphy, M., Stow, N.D., and Preston, V.G. (2006). Herpes simplex virus type 1 DNA-packaging protein UL17 is required for efficient binding of UL25 to capsids. J. Virol. *80*, 2118–2126.

Trus, B.L., Booy, F.P., Newcomb, W.W., Brown, J.C., Homa, F.L., Thomsen, D.R., and Steven, A.C. (1996). The herpes simplex virus procapsid: structure, conformational changes upon maturation, and roles of the triplex proteins VP19c and VP23 in assembly. J. Mol. Biol. *263*, 447–462.

Wakeham, D.E., Chen, C.Y., Greene, B., Hwang, P.K., and Brodsky, F.M. (2003). Clathrin self-assembly involves coordinated weak interactions favorable for cellular regulation. EMBO J. *22*, 4980–4990.

Wills, E., Scholtes, L., and Baines, J.D. (2006). Herpes simplex virus 1 DNA packaging proteins encoded by UL6, UL15, UL17, UL28, and

UL33 are located on the external surface of the viral capsid. J. Virol. *80*, 10894–10899.

Wingfield, P.T., Stahl, S.J., Thomsen, D.R., Homa, F.L., Booy, F.P., Trus, B.L., and Steven, A.C. (1997). Hexon-only binding of VP26 reflects differences between the hexon and penton conformations of VP5, the major capsid protein of herpes simplex virus. J. Virol. *71*, 8955–8961.

Wolfstein, A., Nagel, C.H., Radtke, K., Dohner, K., Allan, V.J., and Sodeik, B. (2006). The inner tegument promotes herpes simplex virus capsid motility along microtubules in vitro. Traffic *7*, 227–237.

Zhou, Z.H., Prasad, B.V., Jakana, J., Rixon, F.J., and Chiu, W. (1994). Protein subunit structures in the herpes simplex virus A-capsid determined from 400 kV spot-scan electron cryomicroscopy. J. Mol. Biol. *242*, 456–469.

Zhou, Z.H., He, J., Jakana, J., Tatman, J.D., Rixon, F.J., and Chiu, W. (1995). Assembly of VP26 in herpes simplex virus-1 inferred from structures of wild-type and recombinant capsids. Nat. Struct. Biol. *2*, 1026–1030.

Zhou, Z.H., Chen, D.H., Jakana, J., Rixon, F.J., and Chiu, W. (1999). Visualization of tegument-capsid interactions and DNA in intact herpes simplex virus type 1 virions. J. Virol. *73*, 3210–3218.

Accession Numbers

The C-capsid density map has been deposited in the Macromolecular Structure Database of the European Bioinformatics Institute (EBI) with accession code EMD-1354.